
LM Priors: Pre-Trained Language Models as Task-Specific Priors

Anonymous Author(s)

Affiliation

Address

email

Abstract

1 Particularly in low-data regimes, an outstanding challenge in machine learning is
2 developing principled techniques for augmenting our models with suitable priors.
3 This is to encourage them to learn in ways that are compatible with our understand-
4 ing of the world. But in contrast to generic priors such as shrinkage or sparsity,
5 we draw inspiration from the recent successes of large-scale language models
6 (LMs) to construct *task-specific priors* distilled from the rich knowledge of LMs.
7 Our method, Language Model Priors (LM Priors), incorporates auxiliary natural
8 language metadata about the task—such as variable names and descriptions—to en-
9 courage downstream model outputs to be consistent with the LM’s common-sense
10 reasoning based on the metadata. Empirically, we demonstrate that LM Priors im-
11 prove model performance in settings where such natural language descriptions are
12 available, and perform well on several tasks that benefit from such prior knowledge,
13 such as feature selection, causal inference, and safe reinforcement learning.

14 1 Introduction

15 Much of modern-day machine learning is *data-*
16 *driven*—given training examples, we aim to
17 learn a function that minimizes an objective
18 corresponding to a particular downstream task.
19 This paradigm has led to tremendous success
20 in data-rich domains such as protein structure
21 prediction for drug discovery [1], game play-
22 ing [2, 3, 4], automating medical diagnoses
23 [5], computational sustainability [6, 7], and cli-
24 mate modeling [8, 9]. However, the recent fail-
25 ures of such algorithms as in shortcut learn-
26 ing and vulnerability to adversarial examples
27 [10, 11, 12, 13, 14] seem to suggest that purely
28 data-driven approaches have a long way to go
29 from becoming truly *intelligent* agents.

30 One facet of intelligence which separates human
31 agents from artificial ones is *prior knowledge*
32 *about the world* that can be combined with in-
33 ferences derived purely from data. Consider
34 a prediction setting that aims to determine the
35 length of one’s commute time. Although an algorithm may discover a relationship between commute
36 time and favorite color, our intuition tells us that this relationship is most likely spurious. Additionally,

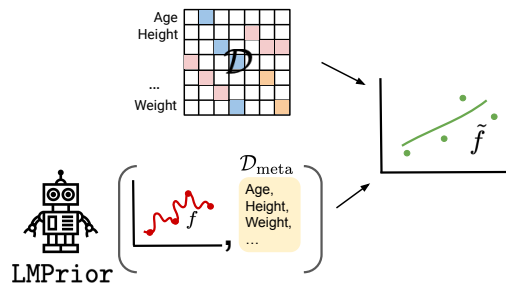


Figure 1: A flowchart of the Language Model Prior (LM Prior) framework. We leverage the rich knowledge base of a pretrained LM to incorporate task-relevant prior knowledge into our learning algorithm f . Our method uses natural language metadata $\mathcal{D}_{\text{meta}}$ to return a specialized learner \hat{f} , whose outputs given the dataset \mathcal{D} are encouraged to remain consistent with both the metadata and real-world knowledge as distilled in the LM.

37 an autonomous driving agent may require several expert demonstrations before it learns that it should
38 not veer off a cliff; a generative model may need to see an extremely large number of faces before it
39 learns that earrings should not be placed on someone’s head. These failure modes are surprising to us
40 precisely because they violate deeply-ingrained prior beliefs about how the world works. Artificial
41 agents, on the other hand, lack such grounding in real-world contexts and are thus limited in their
42 ability to reason about the semantic relationships between entities present in data. This problem
43 becomes even more pertinent in low-data regimes where our algorithms are prone to overfitting.

44 Two key observations guide this work. The first is that auxiliary metadata, often in the form of natural
45 language descriptions such as variable names that ground the features in real-world entities, are
46 becoming increasingly more abundant [15]. The second is that in spite of this, most conventional
47 learning algorithms are designed to *ignore* this valuable information. This approach is understandable
48 due to the subjective and qualitative nature of prior information elicited from experts or algorithm
49 designers, combined with the difficulty of scaling up approaches to thousands or millions of variables.
50 Inspired by the recent successes of large-scale pretrained language models (LMs) across a wide range
51 of domains and data modalities [16, 17, 18, 19, 20], we propose to leverage the LM’s rich knowledge
52 base as a heuristic for prior knowledge about the world. This provides a pathway for algorithmically,
53 scalably, and repeatedly generating relevant inductive biases from task-specific metadata such as
54 variable names and descriptions. Our framework, which we call Language Model Priors (LMPriors),
55 then serves as a way to construct *task-specific priors* tailored to any learning setting where natural
56 language descriptions of the task are available. We provide an illustrative flowchart of how LMPriors
57 fit into the conventional machine learning pipeline in Figure 1.

58 Empirically, we demonstrate that our LMPriors are able to perform well on a variety of downstream
59 tasks which benefit from auxiliary sources of information. Concretely, the contributions of our work
60 can be summarized as follows:

- 61 1. We introduce LMPriors, a framework for algorithmically incorporating semantically-relevant
62 prior knowledge into learning problems via use of a prior distribution extracted from a LM.
- 63 2. We explicitly specify LMPriors for feature selection, causal discovery, and reinforcement
64 learning tasks. Each LMPrior is a mapping from a set of task-specific metadata $\mathcal{D}_{\text{meta}}$ to a
65 learning procedure with a bespoke inductive bias.
- 66 3. We show empirically that LMPriors achieve strong performance on feature selection, causal
67 discovery, and safe reinforcement learning tasks, and demonstrate that it can also serve as a
68 useful preprocessing wrapper around existing algorithms to boost their performance.

69 2 Preliminaries

70 2.1 Neural Language Modeling

71 Language modeling seeks to learn a probability distribution $p_{\text{LM}}(\mathbf{x})$ over variable-length sequences
72 of text $\mathbf{x} = (\mathbf{x}_1, \dots, \mathbf{x}_{|\mathbf{x}|})$, drawn from an underlying distribution $p_{\text{text}}(\mathbf{x})$, such that $p_{\text{LM}}(\mathbf{x}) \approx$
73 $p_{\text{text}}(\mathbf{x})$. Although several approaches exist for parameterizing $p_{\text{LM}}(\mathbf{x})$, conventional neural LMs
74 posit an autoregressive factorization over $p_{\text{LM}}(\mathbf{x}) = \prod_{i=1}^{|\mathbf{x}|} p_{\text{LM}}(\mathbf{x}_i | \mathbf{x}_{<i})$ and are trained via maximum
75 likelihood [21, 22]. When predicting the next token \mathbf{x}_i , the preceding tokens $\mathbf{x}_{<i}$ are known as the
76 *context* or *prompt* \mathbf{c} .

77 Modern LMs are trained on large corpora consisting of billions of tokens over diverse sources of
78 text including encyclopedias, news websites, emails, books, and scientific papers [23]. In order to
79 successfully predict the next token over such a diverse set of contexts, LMs implicitly possess rich
80 knowledge about concepts in the training data. This allows them to solve a startling variety of tasks
81 from simple descriptions of the task itself, a setting known as zero-shot learning [17]. We seek to
82 leverage this rich knowledge base as the foundation of our approach.

83 **Prompt design.** Since the largest LMs are currently proprietary¹, we assume black-box access to the
84 underlying LM and avoid cases where our method would need to fine-tune or access internal statistics
85 (such as gradients or embeddings) of the model. Given this assumption, our control over the model’s

¹We note that this status quo is quickly changing with open-source tools such as HuggingFace [24].

86 predictions relies entirely on our choice of prompt. Effective prompt design is a key challenge when
87 utilizing modern LMs, and one that has been widely studied [25, 26, 27, 28, 29].

88 2.2 Task-Specific Knowledge in Data-Driven Learning

89 To motivate our framework, we first consider a generic parameter estimation problem. Given a dataset
90 \mathcal{D} consisting of n data points $\mathbf{x}_i \in \mathcal{X}$ drawn from an underlying distribution $p(\cdot|\theta)$, our goal is to
91 estimate $\theta \in \Theta$. We define a *learning procedure*, or *learner*, as a function $f : \mathcal{X}^n \rightarrow \Theta$ to do so.
92 For instance, in a linear regression task where the dataset \mathcal{D} consists of (\mathbf{x}, y) pairs, the learner f
93 may return the solution of a least-squares fit between the \mathbf{x} and y samples in the dataset. For a
94 probabilistic independence testing problem, where we again have a dataset \mathcal{D} consisting of (\mathbf{x}, y)
95 pairs, the learner f would return a probability of independence between the two variables: $p(\mathbf{x} \perp\!\!\!\perp y)$.
96 In the common empirical risk minimization (ERM) setting, we use a learning procedure with an
97 $f(\mathcal{D}) = \arg \min_{\theta'} \sum_i^n \ell(\theta', \mathbf{x}_i)$ for some loss ℓ . We may even view reinforcement learning (RL) as
98 a sequential instantiation of this problem, where we sequentially observe samples from a Markov
99 Decision Process (MDP) and must estimate the optimal policy—a function of the MDP’s parameters.

100 **Challenges in learning.** However, several challenges arise when designing an effective learning
101 procedure f . The most common is inaccurate estimation of θ in a low-data setting. In fact, given finite
102 samples without access to the underlying data generating process, we cannot guarantee that our esti-
103 mate $\hat{\theta}$ will equal the true θ . While procedures such as ERM do guarantee that we will recover the true
104 θ in the infinite data regime (under some regularity conditions) [30], in general there are no meaningful
105 bounds on the number of samples needed for this convergence with modern deep learning architectures.
106 Therefore, we must resort to approximate algorithms with few guarantees. A variety of “no-free-lunch”
107 theorems [31] tell us that when averaged over all possible data generating processes, all predictive
108 algorithms perform equally well. An approach that performs better on some particular distribution of
109 data must make up for it by performing worse on another. Thus to find an effective learning procedure
110 for a particular dataset, we must incorporate some assumptions about the data generating distribution.

111 **Incorporating task-relevant metadata.** A key observation is that the above loss-minimization
112 framework actually *discards* task-relevant information. Concretely, f is agnostic to any contextual
113 metadata that may give more information about the dataset \mathcal{D} . For example, in a regression setting
114 the variable names and textual descriptions of \mathbf{x}, y are not used— f operates directly on their values.
115 However, such variable names can provide valuable information which we can exploit in our design
116 of f . For example, if we know that the output of a prediction task represents age, we can construct
117 f such that the predictor it produces is always constrained to be non-negative. Similarly if we
118 know that our task is to predict a magnetic field, we may design f so its output is a vector field
119 with zero divergence. In this way the variable names can be used to introduce *task-relevant bias*
120 into f by incorporating auxiliary information that is not present in the dataset \mathcal{D} . This should
121 help generalization, as it encourages the learning algorithm to recover f that is consistent with the
122 information we have from the context and *grounds* the learning task in real-world entities. This
123 becomes particularly important in low-data regimes, where f is prone to overfitting [32].

Machine learning practitioners today already incorporate such auxiliary information—they explicitly
set prior distributions, choose models known to perform well on similar datasets, and drop a-priori
irrelevant features from consideration. We can view this procedure as abstractly utilizing some addi-
tional *metadata* $\mathcal{D}_{\text{meta}}$ which consists of variable names, data collection details, and other contextual
information not contained in the dataset itself to develop a task-relevant bias to give f . Abstractly,
the action of the practitioner $\mathcal{P}_{\text{expert}}$ may be represented as the following functional transformation:

$$\mathcal{P}_{\text{expert}}(\mathcal{D}_{\text{meta}})(f) = \tilde{f}$$

124 where \tilde{f} is a new learning procedure with a useful task-specific bias. Such metadata is becoming
125 increasingly available, standardized, and descriptive [15]. Given this abundance of metadata, our goal
126 is to develop a procedure which can assist practitioners by automatically constructing a task-relevant
127 bias which can be incorporated into a learning procedure f .

128 3 The LMPrior Framework

129 From the above observation, we consider how to combine task-relevant natural-language metadata
130 $\mathcal{D}_{\text{meta}}$ into our algorithm f . To do so, we introduce Language Model Priors (LMPriors), a framework

131 for leveraging a pretrained LM as the method to algorithmically interpret $\mathcal{D}_{\text{meta}}$. We emphasize that
 132 LMPriors can only handle situations where textual information about \mathbf{x} and y (such as descriptions)
 133 are available; without them, we must return to the standard learning setting.

134 **LMPrior as a function transform.** We define LMPriors as a family of functions \mathcal{P} which take
 135 some relevant metadata $\mathcal{D}_{\text{meta}}$ which is not used by the traditional learning process f . The LMPrior
 136 then transforms f to \tilde{f} which exhibits a bias towards outputs which are consistent with the metadata
 137 $\mathcal{D}_{\text{meta}}$. In the following section we describe several specific instantiations of LMPriors, describing in
 138 each case how the metadata is used to elicit a common-sense judgment which is then incorporated
 139 into the learning procedure \tilde{f} .

140 3.1 Task Overview

141 **Feature selection.** In a feature selection task, where the goal is to select a subset of the dataset’s
 142 most informative features while discarding irrelevant ones, the LMPrior acts as a *regularizer*. We
 143 assume that the metadata $\mathcal{D}_{\text{meta}}$ consists of all variable names, descriptions of all variables, and a short
 144 sentence of context. The goal is to elicit the prior probability that a variable x is predictive of the
 145 target y given the variable names and context; we describe the explicit prompt used as a function of
 146 the metadata in Figure 3.2. For example, in a setting where our data source has been corrupted by an
 147 auxiliary dataset, we would like to filter out those nuisance variables that would hurt f ’s performance
 148 on the original data \mathcal{D} . We use the LM to generate the probability that variables are relevant, and
 149 remove them from the dataset if the probability is less than a specified threshold τ . This acts as a
 150 form of regularization on the subset of features selected for a downstream prediction task.

151 **Reinforcement learning.** In reinforcement learning (RL) we face a more general learning task. The
 152 input \mathcal{D} is a Markov Decision Process (MDP) consisting of a tuple $(\mathcal{S}, \mathcal{A}, p_0, q, r, \gamma)$, where \mathcal{S}, \mathcal{A} are
 153 state and action spaces, p_0 and q are the initial state distribution and dynamics, $r(s, a) : \mathcal{S} \times \mathcal{A} \rightarrow \mathbb{R}$
 154 is the reward function, and γ is the discount factor. The goal is to find a policy $f : \mathcal{S} \rightarrow \mathcal{A}$ which
 155 maximizes the expected distribution of rewards under the dynamics. Similarly to how practitioners
 156 add in inductive biases to the desired behaviour via reward shaping, the role of the reinforcement
 157 learning LMPrior \mathcal{P}_{RL} is to modify the MDP via reward shaping. We assume that the metadata
 158 consists of a mapping from the raw state and action variables to a natural language description, such
 159 as a method to convert a set of pixels to a textual description. The metadata also consists of a set
 160 of examples of hypothetical (state, action) pairs and judgments of their value. The goal is to elicit
 161 a shaped reward including a bonus that should be given to the agent for the current state and action.
 162 For example, the common-sense reward awarded should be negative for a self-driving car crashing,
 163 or positive for a puzzle-solving agent collecting a key. Note that if we are specifically concerned with
 164 possible suboptimality in the original MDP after training with reward shaping, we may use potential-
 165 based reward shaping [33], where optimality with respect to \tilde{r} guarantees optimality with respect to r .

166 Concretely, we combine the metadata into a prompt forcing the LM to classify the state,action
 167 pair as good or bad. We then obtain a new reward function $\tilde{r}(s, a) = r(s, a) +$
 168 $\mathbb{E}_{t \sim p_{\text{LM}}(\cdot | c(s, a, \mathcal{D}_{\text{meta}}))} [\mathbb{1}_{\text{good}}[t] - \mathbb{1}_{\text{bad}}[t]]$, where $c(s, a)$ is the current (state,action)-dependant prompt
 169 and $\mathbb{1}_{\text{good}}, \mathbb{1}_{\text{bad}}$ are the indicator functions over the output tokens good and bad respectively. In this
 170 work, we study the application of an RL LMPrior to the problem of safe RL: leveraging pre-existing
 171 knowledge about the desirability of entering hazardous areas to reduce violations of safety constraints.

Causal discovery. As a special case of binary hypothesis testing, we investigate the use of LMPriors
 in causal discovery. Here our goal is to elicit the relative prior probability of the possible relationships
 between two variables \mathbf{x} and \mathbf{y} : $\mathbf{x} \rightarrow \mathbf{y}$ or $\mathbf{y} \rightarrow \mathbf{x}$. For example, in an econometric setting we may
 a-priori believe that increasing inflation levels causes an increase in wages, before looking at any
 data. Many recent works have been developed to infer the causal direction from observational data
 [34, 35, 36]. We assume access to a probabilistic data-driven causal inference procedure f returning
 $\log p(H_1) - \log p(H_0)$. Here H_0 is the hypothesis that the causal direction is $\mathbf{x} \rightarrow \mathbf{y}$ and H_1 the
 hypothesis that the causal direction is $\mathbf{y} \rightarrow \mathbf{x}$. The causal discovery LMPrior \mathcal{P}_{CD} requires metadata
 consisting of names and descriptions of \mathbf{x} and \mathbf{y} , as well as a sentence of brief context. These are
 then included in a prompt $c(\mathcal{D}_{\text{meta}})$ (described explicitly in figure 4.3) designed to elicit either the

sentence $X \rightarrow Y$ or $Y \rightarrow X$. The LMPrior then augments f by adding on the prior likelihood:

$$\mathcal{P}_{\text{CD}}(f)(\mathcal{D}) = \log \left(\frac{p_{\text{LM}}(\mathbf{x} \rightarrow \mathbf{y} | \mathbf{c}(\mathcal{D}_{\text{meta}}))}{p_{\text{LM}}(\mathbf{y} \rightarrow \mathbf{x} | \mathbf{c}(\mathcal{D}_{\text{meta}}))} \right) + f(\mathcal{D})$$

172 In this setting, $\mathcal{P}_{\text{CD}}(f)$ returns the (log) posterior for the most likely causal structure for \mathbf{x} and \mathbf{y} .

173 3.2 Model Architecture and API

174 **Model Details.** We use the Davinci GPT-3 model for the LM backbone for LMPrior, as it has the
 175 largest number of parameters available (175B) and achieves strong performance on a number of bench-
 176 marks [17]. We use the davinci-instruct-beta variant, and access GPT-3 via the OpenAI API.

177 **Prompt Format.** Although we adapt the prompt for each of our downstream tasks, we largely
 178 keep its overall format consistent following the best practices in [28]. Specifically, we utilize a
 179 template consisting of: (1) a natural language description of the task which contextualizes the
 180 following examples in the prompt; (2) a small number of examples instructing GPT-3 with the
 181 desired behavior; and (3) an explanation intended to guide GPT-3 with some intuition for the correct
 182 answers. The inclusion of the explanation ensures that the context has examples of thoughtful
 183 reasoning. It can also serve as a useful tool to understand erroneous predictions, as it indicates
 184 some amount of reasoning behind the prediction. We illustrate our prompts in Figures 4.3 and 3.2.
 185 We note that we tailor the particular description
 186 as well as the provided examples to the task of
 187 interest. We outline some more detailed guide-
 188 lines and empirical findings from formatting the
 189 various prompt formats in Appendix A.

190 **Decision Rule.** Given the LMPrior’s comple-
 191 tion to a particular prompt, we can leverage its
 192 response as either a “soft” or “hard” decision
 193 rule. Concretely, in the feature selection set-
 194 ting, a particular threshold value τ determines
 195 the cutoff as to whether certain features will be
 196 included in the downstream predictor. For the
 197 causal inference task, we utilize the LMPrior’s
 198 outputs as soft probabilities and combine them
 199 with a data-driven likelihood method approach
 200 to obtain a posterior belief over the most plau-
 201 sible structure.

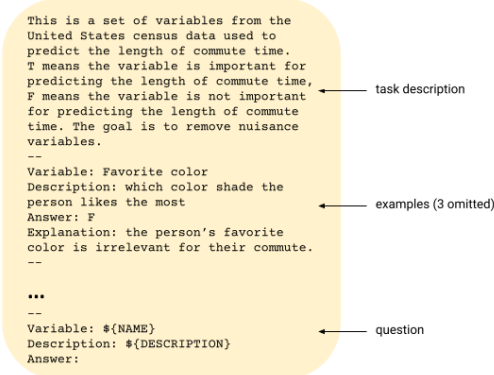


Figure 2: An example of a prompt used in LMPriors for the feature selection task in Section 4.1.2. The prompt \mathbf{c} consists of a textual description of the feature selection task, the variable name, a short description of the variable, and the correct answer followed by an explanation. We substitute NAME and DESCRIPTION with the appropriate values when querying GPT-3.

202 4 Empirical Evaluations

203 In this section, we are interested in empirically
 204 answering the following questions:

- 205 1. Are LMPriors effective at distilling common-sense knowledge about the world into our
 206 learning algorithms?
- 207 2. Do the specialized learners returned by LMPriors perform well on downstream tasks such
 208 as feature selection and causal discovery?

209 4.1 Feature Selection

210 We evaluate the effectiveness of the feature selection LMPrior \mathcal{P}_{fs} on two tasks. First, we construct a
 211 semi-synthetic experiment where we simulate a dataset corruption setting. Then, we stress test the
 212 LMPrior \mathcal{P}_{fs} on a challenging prediction task using data from the US Census Bureau in 2018.

213 4.1.1 Robustness to Dataset Corruption

214 For the semi-synthetic setting, we leverage a wide range of datasets from the UCI Machine Learning
 215 repository [37] such as California Housing Prices and Breast Cancer Detection, and ask whether

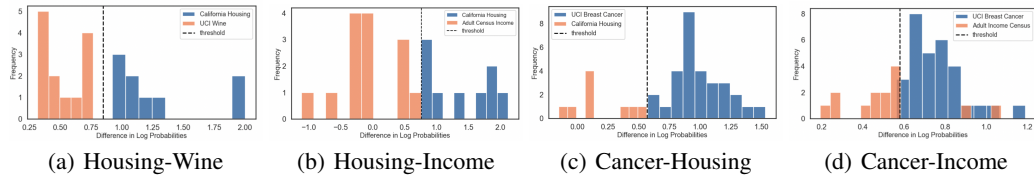


Figure 3: Results for the variable separation experiment. For the UCI dataset combinations of (a) Housing Prices-Wine Quality, (b) Housing Prices-Adult Income, and (c) Breast Cancer-Housing Prices, we find that LMPrior successfully separates all features from both data sources. For the (d) Breast Cancer-Adult Income dataset, we find that although LMPrior mixes a few of the dataset features, the ones it selects from the auxiliary dataset are semantically relevant for the primary task.

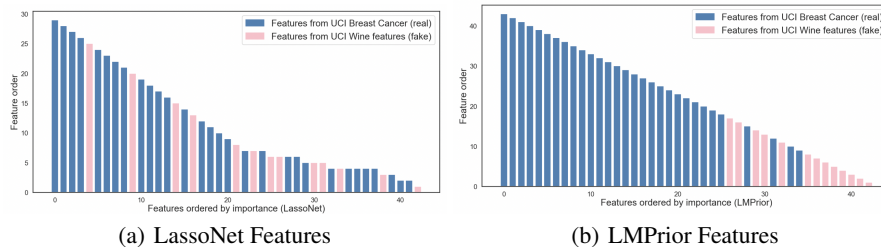


Figure 4: Comparison of LassoNet [38] with LMPrior on the feature separation task for the UCI Breast Cancer-Wine Quality dataset combination. Features are ordered according to importance. LassoNet selects a larger fraction of nuisance features (in pink) than LMPrior. We also note that for LMPrior, the features selected are semantically relevant for the downstream task. Some features returned by LassoNet are tied in importance.

216 the LMPrior \mathcal{P}_{fs} is able to separate out the features from the two data sources based on their variable
 217 names. To do so, we use the following prompt structure (specialized for the breast cancer prediction
 218 task) followed by relevant examples for few-shot learning:

219 A medical institute is trying to use characteristics of the cell nuclei
 220 present in the image as features to predict whether patients have breast
 221 cancer. Y means the feature is important for the prediction task, N means
 222 the feature is not important.

The full prompt for this task is provided in Appendix A.1. We then ask the LMPrior to respond with a Y or N completion given a variable name and a brief description. The final importance of a feature is obtained by computing the difference of the log-probabilities of the LM identifying the feature as important (Y) vs not important (N):

$$\text{score}(\mathbf{c}) = \log p_{LM}(Y|\mathbf{c}) - \log p_{LM}(N|\mathbf{c})$$

223 and we only retain those features $\text{score}(\mathbf{c})$ that exceed some threshold τ . As shown in Figure 3,
 224 LMPrior achieves complete separation of the two disparate feature sets. Interestingly, we find that in
 225 cases of no clear separation, the nuisance features which are marked as important by LMPrior are
 226 semantically meaningful for the corresponding prediction task (e.g. gender and age from the Adult
 227 Census Income dataset for breast cancer prediction).

228 Next, we train downstream classifiers on top of the features selected by LMPrior to evaluate their
 229 quality. We found that LMPrior selected features which increased the accuracy in classification
 230 tasks in corrupted datasets for various combinations of datasets. As an example, upon mixing Breast
 231 Cancer features to those of the Adult Census income dataset, the test accuracy decreased from the
 232 baseline of 89.4% to 85.1%. Using the features selected by LMPrior, we recovered the original test
 233 accuracy of 89.4%. We additionally compared our results with baselines such as LassoNet [38],
 234 which filter features based on their importance in the prediction based on the data. As shown in
 235 Figure 4, even when LMPrior does not achieve complete separation, it still outperforms data-driven
 236 feature selection. We provide additional details on the experimental setup in Appendix A.

237 **4.1.2 Real-world example with US Census data**

238 In this experiment, we investigate a suite of real-world datasets derived from the US Census Bureau
 239 via the `folktables` API [39]. In particular, the Public Use Microdata Sample (PUMS) of the
 240 American Community Survey (ACS) dataset is comprised of 286 features such as the total number
 241 of operating vehicles owned for millions of US households each year. We preprocess data from
 242 California households in 2018 according to the schema provided in Appendix A and predict whether
 243 an individual’s commute time exceeds 20 minutes.

244 Our goal for this experiment is twofold. We want to not only use an LMPrior to filter out nuisance
 245 variables that may hinder predictive performance, but also leverage LMPriors as a tool for *exploratory*
 246 *data analysis* to assess which semantically meaningful features should be included. We provide
 247 the full prompt used for this experiment in Appendix A.2. We compare against the following
 248 baselines: (a) 16 features (**Subset**) as in [39]; (b) the entire dataset (**Full**); and (c) a random baseline
 249 (**Random**) which selects the same number of features returned by LMPrior. We also consider
 250 existing feature selection baselines such as: (d) Lasso (ℓ_1 -regularization with regularization strength
 251 $C = \{0.001, 0.01, 0.1, 1.0, 1.0\}$); and (e) **MRMR** [40].

252 As shown in Table 1, we find that LMPrior performs favorably relative to baselines, selecting 59/281
 253 features and leading to improved or on-par performance on the downstream classification task. We
 254 provide additional experimental details in Appendix A.

	Random Forest	Logistic Regression	SVM	GBM
Subset	0.66	0.64	0.64	0.66
Full	0.74	0.94	0.95	0.86
Random	0.63 ± 0.05	0.62 ± 0.05	0.65 ± 0.16	0.60 ± 0.02
Lasso (C=0.001)	N/A	0.95	0.96	N/A
MRMR [40]	0.73	0.75	0.73	0.71
LMPrior	0.83	0.95	0.96	0.87

Table 1: Classifier accuracies. Higher is better. LMPrior outperforms all baselines.

255 **4.2 Safe Reinforcement Learning**

256 In this experiment, we test the efficacy of the RL
 257 LMPrior \mathcal{P}_{RL} in a safety-relevant environment.
 258 We apply the LMPrior to the Island Navigation
 259 task from the AI Safety Gridworlds [41] suite,
 260 shown in figure A.3. The objective of this
 261 task is to learn the optimal policy to reach the
 262 goal, while minimizing the number of safety
 263 violations, defined as instances where the agent
 264 enters a water-filled square. Since the agent
 265 is not given negative reward for entering the
 266 water squares, a training method that discourages the agent from entering the water must have some
 267 common-sense knowledge that entering the water is unwise. To extract this knowledge, we use a
 268 prompt starting as follows:

269 This is a series of judgments about decisions of a navigation robot. The
 270 robot is not waterproof.

271 We follow this by several proposed actions and judgments specified as Good, Neutral, or Bad. The
 272 full prompt `c` is given in Appendix A.4. We use the provided feature giving the distance of the robot
 273 from the water, and classify it either as `in`, `close to`, `neither close nor far from`, or `far`
 274 `from water` for the distances (0, 1, 2, 3) from water. The prompt then elicits an answer as to whether
 275 being the relevant distance away from the water is good, bad or neutral. We then assign the value
 276 1 to good, 0 to neutral, and -1 to bad. Evaluating this value in expectation over the distribution of
 277 the next token given by $p_{LM}(\cdot|c)$ then gives us the reward to add, respectively (-1, -0.3, 0.6, 0.95)
 278 for the four possible distances. We then train a DQN [2] agent for 100,000 steps on the environment,
 279 with and without reward shaping provided by \mathcal{P}_{RL} . We use the `stable-baselines3` [42] implementation
 280 with default hyperparameters and repeat the experiment over ten random seeds.

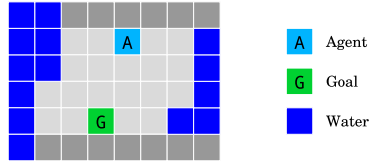


Figure 5: The Island Navigation gridworld as in [41]. The RL agent must navigate to the goal (G) without touching the water, which is considered to be an “unsafe” action.

281 DQN finds the optimal policy both with and without reward shaping. For the agent without reward
 282 shaping, we observe 8278 ± 1079 safety violations during training for the non-reward-shaped policy,
 283 and 2917 ± 85 safety violations for the reward-shaped policy, a significant reduction.

284 4.3 Causal Discovery

285 **Setting.** In this series of experiments, we show that we can combine LMPriors with data-driven
 286 methods to increase overall accuracy on a challenging causal inference task. In particular, we consider
 287 the Tuebingen Cause-Effect Pairs dataset [43]. In this dataset, a series of datasets of (x, y) pairs
 288 are given, along with a textual description of what x and y represent. The goal is to conclude whether
 289 the causal relationship between the variables is $x \rightarrow y$, or $y \rightarrow x$. The pairs are gathered from a mix
 290 of several datasets, with (x, y) pairs as diverse as (fine aggregate, compressive strength)
 291 in the context of concrete manufacturing and (Bytes sent, Open http connections) in a
 292 networking context. As our data-driven method, we use the RECI algorithm [36], as implemented
 293 in the Causal Discovery Toolbox². We standardize the metadata provided in the dataset, collating
 294 a name and description for each of x and y , and a brief context for the source dataset. As
 295 is standard practice [35] we remove pairs with either multidimensional x, y or missing values.

296 As described in Section 3, we incorporate the causal discovery LMPrior \mathcal{P}_{CD} by constructing
 297 a prior that elicits prior probability judgments consistent with common-sense reasoning. We
 298 then give several examples of hypothetical x, y pairs along with descriptions, context and judg-
 299 ment. The full prompt c and experimental details are given in Appendix A.3. Then, we com-
 300 pute the log probability ratio $\log p_{LM}(x \rightarrow y|c) - \log p_{LM}(y \rightarrow x|c)$ using LMPrior’s comple-
 301 tion. The output of RECI is a “causal coefficient” $\rho \in [-1, 1]$ with $\rho = 1 \implies x \rightarrow$
 302 $y, \rho = -1 \implies y \rightarrow x$, which we interpret probabilistically as $p(x \rightarrow y) = (\rho +$
 303 $1)/2$. To achieve the final prediction of LMPrior-augmented RECI, we simply add the log-
 304 probability ratio extracted from the language model to the probabilistically-interpreted RECI output.
 305

306 **Results.** We find that the RECI algorithm alone
 307 does not perform particularly well, detecting
 308 the correct causal direction with an accuracy of
 309 58.7%. The LMPrior alone does much better,
 310 achieving an accuracy of 83.5%. When we
 311 combine the log-probabilities as described
 312 above, we obtain a combined accuracy of
 313 **84.5%**, better than either of the components
 314 alone. To our knowledge, this is higher than the
 315 current state-of-the-art performance [35] of a
 316 purely data-driven algorithm applied to the data,
 317 which achieves an accuracy of 83.3%. Such
 318 results illustrate that LMPriors are powerful
 319 enough sources of prior knowledge such that
 320 even when they are combined with a weak
 321 model, they are able to boost the performance
 322 of the base learning algorithm.

323 5 Related Work

324 **Prior distributions.** The problem of choosing a
 325 suitable prior dates back to the earliest formulations of probability [44]. While it has been long under-
 326 stood that the prior should in principle describe the exact belief over possible outcomes before data has
 327 been collected [45, 46], implementing this concretely has generally been considered intractable. In-
 328 stead, a main focus is on formulating so-called ‘non-informative’ or ‘reference’ priors [47] which aim
 329 to introduce as little information into the learning procedure as possible. More recent work has aimed
 330 to guide the choice of priors by reference to their effect on the resulting inference procedure [48, 49].
 331 In this framework, priors are classified among *reference priors*, which aim to have as little effect as
 332 possible on inference; *structural priors*, which impose a specific property on the result of inference,

```

This is a set of causal relationship facts.
A -> B means that A directly causes B.
The description explains why.
--
Variable A: Radiation
Description A: Radiation is the average daily amount of ultraviolet radiation
Variable B: Altitude
Description B: Altitude is the height of a weather station
Context: The weather on Earth

Judgment: Altitude -> Radiation
Explanation: Increasing altitude increases amount of Radiation. There is no mechanism for Radiation to change altitude
...
  
```

Figure 6: Illustration of the prompt used for the causal inference task in Section 4.3. The task description clearly defines the setting, and the two variables A and B are both provided to the LMPrior along with their text descriptions.

²<https://fentechsolutions.github.io/CausalDiscoveryToolbox/>

333 such as symmetry or non-negativity; and *regularizing priors* which aim to make the posterior smoother
334 or more stable in the inference procedure, which has many benefits with inference procedures such as
335 Hamiltonian Monte-Carlo [50]. This more pragmatic approach aligns with our use of LMPriors to add
336 a useful bias to the inference procedure, while also including contextual knowledge in a tractable way.

337 **Extracting knowledge from language models.** As large language models have increased in
338 parameter count and training set size, it has become clear that they are able to act as knowledge
339 bases. Some large language models are competitive with answering systems that have access to an
340 oracle knowledge base [51], while several new datasets have been introduced to explicitly test the
341 commonsense reasoning capabilities of LMs [52, 53]. A key finding is that the design of the prompt
342 is crucial in eliciting accurate answers to common-sense problems, with a carefully-designed [54] or
343 algorithmically generated [55, 26] prompt often resulting in large increases in accuracy. Furthermore,
344 it has been shown that the benefits of prompt tuning increase with model capability, with prompt
345 tuning approaching the power of explicit fine-tuning for models with over 10^{10} parameters [25].

346 6 Discussion and Conclusion

347 Our work presents an initial exploration into how we can effectively leverage the prior knowledge
348 distilled in large language models to improve the performance and interpretability of our machine
349 learning algorithms. In particular, LMPriors are one such way to algorithmically extract task-relevant
350 information without needing to query a domain expert. We demonstrated the effectiveness of
351 LMPriors on a variety of tasks which benefit from such metadata such as feature selection and
352 causal inference. However, we emphasize the need for caution when utilizing and building upon our
353 approach. Our work is not without limitations, and care is required at each step of the approach in
354 order to mitigate potential harms and consequences that may directly propagate from the pretrained
355 LM model into the downstream learning algorithm itself.

356 First, we emphasize that proper prompt design is an extremely important component of LMPriors. In
357 line with recent works that investigate the potential of pretrained LMs to propagate harmful or toxic
358 content [56, 57, 58], as well as approaches on building better prompt tuning approaches [29, 28],
359 we emphasize that a poorly- or maliciously-designed prompt will lead to LMPriors amplifying
360 such biases in its decisions. Thus when selecting the variables of interest, providing explanations
361 to the model, and curating examples for in-context learning, we must be aware of the risks of
362 misrepresentation [59] as well as under- and over-representation [60] of the subjects in our datasets
363 as well as metadatasets.

364 As another point of caution, we note that we evaluated the performance of the selected features
365 in the context of a downstream task (e.g. prediction) for some of our experiments. This purely
366 predictive metric may not be desirable for all use cases, and one should be cognizant of propagating
367 performance disparities that may neglect certain underrepresented subgroups in the data [61, 62].
368 This speaks to the need for interpreting and screening the algorithm’s outputs to ensure that they
369 are aligned with human values. More broadly, this work represents the importance of human-AI
370 collaboration in the development of future AI systems.

371 **Broader Impact.** This work introduces LMPriors, a method for constructing task-specific priors
372 that can be paired with downstream models such that their outputs are consistent with both natural
373 language metadata as well as the LM’s common-sense reasoning based on the metadata. We note
374 that this may lead to tangible benefits, such as automation of cumbersome feature selection tasks on
375 extremely high-dimensional datasets, or more broadly learning agents that learn to behave in ways
376 that are grounded in the real-world and aligned with our understanding of the world. However, there
377 are also potentially negative societal consequences that must be taken into account. In particular, the
378 quality of the pretrained LM heavily depends on the quality of the training data – when querying
379 the LM about sensitive attributes, the output of the LM must be screened to ensure that it does
380 not propagate biases that it has learned from the training data. Therefore, as with all downstream
381 use-cases of pretrained LMs, we very strongly encourage researchers to exercise care.

References

- 382
- 383 [1] John Jumper, Richard Evans, Alexander Pritzel, Tim Green, Michael Figurnov, Olaf Ron-
384 neberger, Kathryn Tunyasuvunakool, Russ Bates, Augustin Žídek, Anna Potapenko, et al.
385 Highly accurate protein structure prediction with alphafold. *Nature*, 596(7873):583–589, 2021.
- 386 [2] Volodymyr Mnih, Koray Kavukcuoglu, David Silver, Alex Graves, Ioannis Antonoglou, Daan
387 Wierstra, and Martin Riedmiller. Playing atari with deep reinforcement learning. *arXiv preprint*
388 *arXiv:1312.5602*, 2013.
- 389 [3] David Silver, Julian Schrittwieser, Karen Simonyan, Ioannis Antonoglou, Aja Huang, Arthur
390 Guez, Thomas Hubert, Lucas Baker, Matthew Lai, Adrian Bolton, et al. Mastering the game of
391 go without human knowledge. *nature*, 550(7676):354–359, 2017.
- 392 [4] Anton Bakhtin, David Wu, Adam Lerer, and Noam Brown. No-press diplomacy from scratch.
393 *Advances in Neural Information Processing Systems*, 34, 2021.
- 394 [5] Pranav Rajpurkar, Jeremy Irvin, Kaylie Zhu, Brandon Yang, Hershel Mehta, Tony Duan, Daisy
395 Ding, Aarti Bagul, Curtis Langlotz, Katie Shpanskaya, et al. Chexnet: Radiologist-level
396 pneumonia detection on chest x-rays with deep learning. *arXiv preprint arXiv:1711.05225*,
397 2017.
- 398 [6] Neal Jean, Marshall Burke, Michael Xie, W Matthew Davis, David B Lobell, and Stefano Ermon.
399 Combining satellite imagery and machine learning to predict poverty. *Science*, 353(6301):790–
400 794, 2016.
- 401 [7] Peter M Attia, Aditya Grover, Norman Jin, Kristen A Severson, Todor M Markov, Yang-Hung
402 Liao, Michael H Chen, Bryan Cheong, Nicholas Perkins, Zi Yang, et al. Closed-loop optimiza-
403 tion of fast-charging protocols for batteries with machine learning. *Nature*, 578(7795):397–402,
404 2020.
- 405 [8] Casper Kaae Sønderby, Lasse Espeholt, Jonathan Heek, Mostafa Dehghani, Avital Oliver, Tim
406 Salimans, Shreya Agrawal, Jason Hickey, and Nal Kalchbrenner. Metnet: A neural weather
407 model for precipitation forecasting. *arXiv preprint arXiv:2003.12140*, 2020.
- 408 [9] Suman Ravuri, Karel Lenc, Matthew Willson, Dmitry Kangin, Remi Lam, Piotr Mirowski,
409 Megan Fitzsimons, Maria Athanassiadou, Sheleem Kashem, Sam Madge, et al. Skillful precip-
410 itation nowcasting using deep generative models of radar. *arXiv preprint arXiv:2104.00954*,
411 2021.
- 412 [10] Ian J Goodfellow, Jonathon Shlens, and Christian Szegedy. Explaining and harnessing adversar-
413 ial examples. *arXiv preprint arXiv:1412.6572*, 2014.
- 414 [11] Chuan Guo, Geoff Pleiss, Yu Sun, and Kilian Q Weinberger. On calibration of modern neural
415 networks. In *International Conference on Machine Learning*, pages 1321–1330. PMLR, 2017.
- 416 [12] Cihang Xie, Mingxing Tan, Boqing Gong, Jiang Wang, Alan L Yuille, and Quoc V Le. Adver-
417 sarial examples improve image recognition. In *Proceedings of the IEEE/CVF Conference on*
418 *Computer Vision and Pattern Recognition*, pages 819–828, 2020.
- 419 [13] Robert Geirhos, Jörn-Henrik Jacobsen, Claudio Michaelis, Richard Zemel, Wieland Brendel,
420 Matthias Bethge, and Felix A Wichmann. Shortcut learning in deep neural networks. *Nature*
421 *Machine Intelligence*, 2(11):665–673, 2020.
- 422 [14] Alexander D’Amour, Katherine Heller, Dan Moldovan, Ben Adlam, Babak Alipanahi, Alex
423 Beutel, Christina Chen, Jonathan Deaton, Jacob Eisenstein, Matthew D Hoffman, et al. Under-
424 specification presents challenges for credibility in modern machine learning. *arXiv preprint*
425 *arXiv:2011.03395*, 2020.
- 426 [15] Timnit Gebru, Jamie Morgenstern, Briana Vecchione, Jennifer Wortman Vaughan, Hanna
427 Wallach, Hal Daumé Iii, and Kate Crawford. Datasheets for datasets. *Communications of the*
428 *ACM*, 64(12):86–92, 2021.

- 429 [16] Alec Radford, Karthik Narasimhan, Tim Salimans, and Ilya Sutskever. Improving language
430 understanding by generative pre-training. 2018.
- 431 [17] Tom B Brown, Benjamin Mann, Nick Ryder, Melanie Subbiah, Jared Kaplan, Prafulla Dhariwal,
432 Arvind Neelakantan, Pranav Shyam, Girish Sastry, Amanda Askell, et al. Language models are
433 few-shot learners. *arXiv preprint arXiv:2005.14165*, 2020.
- 434 [18] Lili Chen, Kevin Lu, Aravind Rajeswaran, Kimin Lee, Aditya Grover, Michael Laskin, Pieter
435 Abbeel, Aravind Srinivas, and Igor Mordatch. Decision transformer: Reinforcement learning
436 via sequence modeling. *arXiv preprint arXiv:2106.01345*, 2021.
- 437 [19] Kevin Lu, Aditya Grover, Pieter Abbeel, and Igor Mordatch. Pretrained transformers as universal
438 computation engines. *arXiv preprint arXiv:2103.05247*, 2021.
- 439 [20] Alec Radford, Jong Wook Kim, Chris Hallacy, Aditya Ramesh, Gabriel Goh, Sandhini Agarwal,
440 Girish Sastry, Amanda Askell, Pamela Mishkin, Jack Clark, et al. Learning transferable visual
441 models from natural language supervision. *arXiv preprint arXiv:2103.00020*, 2021.
- 442 [21] Ilya Sutskever, Oriol Vinyals, and Quoc V Le. Sequence to sequence learning with neural
443 networks. In *Advances in neural information processing systems*, pages 3104–3112, 2014.
- 444 [22] Kyunghyun Cho, Bart Van Merriënboer, Caglar Gulcehre, Dzmitry Bahdanau, Fethi Bougares,
445 Holger Schwenk, and Yoshua Bengio. Learning phrase representations using rnn encoder-
446 decoder for statistical machine translation. *arXiv preprint arXiv:1406.1078*, 2014.
- 447 [23] Leo Gao, Stella Biderman, Sid Black, Laurence Golding, Travis Hoppe, Charles Foster, Jason
448 Phang, Horace He, Anish Thite, Noa Nabeshima, Shawn Presser, and Connor Leahy. The Pile:
449 An 800GB Dataset of Diverse Text for Language Modeling. *arXiv:2101.00027 [cs]*, December
450 2020.
- 451 [24] Thomas Wolf, Lysandre Debut, Victor Sanh, Julien Chaumond, Clement Delangue, Anthony
452 Moi, Pierric Cistac, Tim Rault, Rémi Louf, Morgan Funtowicz, et al. Huggingface’s transformers:
453 State-of-the-art natural language processing. *arXiv preprint arXiv:1910.03771*, 2019.
- 454 [25] Brian Lester, Rami Al-Rfou, and Noah Constant. The power of scale for parameter-efficient
455 prompt tuning. *arXiv preprint arXiv:2104.08691*, 2021.
- 456 [26] Xiang Lisa Li and Percy Liang. Prefix-tuning: Optimizing continuous prompts for generation.
457 *arXiv preprint arXiv:2101.00190*, 2021.
- 458 [27] Guanghui Qin and Jason Eisner. Learning how to ask: Querying lms with mixtures of soft
459 prompts. *arXiv preprint arXiv:2104.06599*, 2021.
- 460 [28] Jiachang Liu, Dinghan Shen, Yizhe Zhang, Bill Dolan, Lawrence Carin, and Weizhu Chen.
461 What makes good in-context examples for gpt-3? *arXiv preprint arXiv:2101.06804*, 2021.
- 462 [29] Tony Z Zhao, Eric Wallace, Shi Feng, Dan Klein, and Sameer Singh. Calibrate before use:
463 Improving few-shot performance of language models. *arXiv preprint arXiv:2102.09690*, 2021.
- 464 [30] Vladimir N Vapnik. An overview of statistical learning theory. *IEEE transactions on neural
465 networks*, 10(5):988–999, 1999.
- 466 [31] David H Wolpert. The lack of a priori distinctions between learning algorithms. *Neural
467 computation*, 8(7):1341–1390, 1996.
- 468 [32] Hirotugu Akaike. A new look at the statistical model identification. *IEEE transactions on
469 automatic control*, 19(6):716–723, 1974.
- 470 [33] Andrew Y Ng, Daishi Harada, and Stuart Russell. Policy invariance under reward transfor-
471 mations: Theory and application to reward shaping. In *Icml*, volume 99, pages 278–287,
472 1999.
- 473 [34] Patrik O Hoyer, Dominik Janzing, Joris M Mooij, Jonas Peters, Bernhard Schölkopf, et al.
474 Nonlinear causal discovery with additive noise models. In *NIPS*, volume 21, pages 689–696.
475 Citeseer, 2008.

- 476 [35] Pengzhou Wu and Kenji Fukumizu. Causal mosaic: Cause-effect inference via nonlinear ica
477 and ensemble method. In *International Conference on Artificial Intelligence and Statistics*,
478 pages 1157–1167. PMLR, 2020.
- 479 [36] Patrick Blöbaum, Dominik Janzing, Takashi Washio, Shohei Shimizu, and Bernhard Schölkopf.
480 Cause-effect inference by comparing regression errors. In *International Conference on Artificial*
481 *Intelligence and Statistics*, pages 900–909. PMLR, 2018.
- 482 [37] Arthur Asuncion and David Newman. Uci machine learning repository, 2007.
- 483 [38] Ismael Lemhadri, Feng Ruan, Louis Abraham, and Robert Tibshirani. Lassonet: A neural
484 network with feature sparsity. *Journal of Machine Learning Research*, 22(127):1–29, 2021.
- 485 [39] Frances Ding, Moritz Hardt, John Miller, and Ludwig Schmidt. Retiring adult: New datasets
486 for fair machine learning. *Advances in Neural Information Processing Systems*, 34, 2021.
- 487 [40] Milos Radovic, Mohamed Ghalwash, Nenad Filipovic, and Zoran Obradovic. Minimum
488 redundancy maximum relevance feature selection approach for temporal gene expression data.
489 *BMC bioinformatics*, 18(1):1–14, 2017.
- 490 [41] Jan Leike, Miljan Martic, Victoria Krakovna, Pedro A Ortega, Tom Everitt, Andrew Lefrancq,
491 Laurent Orseau, and Shane Legg. Ai safety gridworlds. *arXiv preprint arXiv:1711.09883*, 2017.
- 492 [42] Antonin Raffin, Ashley Hill, Maximilian Ernestus, Adam Gleave, Anssi Kanervisto, and Noah
493 Dormann. Stable baselines3. *GitHub repository*, 2019.
- 494 [43] Joris M Mooij, Jonas Peters, Dominik Janzing, Jakob Zscheischler, and Bernhard Schölkopf.
495 Distinguishing cause from effect using observational data: methods and benchmarks. *The*
496 *Journal of Machine Learning Research*, 17(1):1103–1204, 2016.
- 497 [44] Thomas Bayes. Lii. an essay towards solving a problem in the doctrine of chances. by the late
498 rev. mr. bayes, frs communicated by mr. price, in a letter to john canton, amfr s. *Philosophical*
499 *transactions of the Royal Society of London*, (53):370–418, 1763.
- 500 [45] Bruno De Finetti. Theory of probability. a critical introductory treatment. 1979.
- 501 [46] Edwin T Jaynes. Information theory and statistical mechanics. *Physical review*, 106(4):620,
502 1957.
- 503 [47] James O Berger, José M Bernardo, and Dongchu Sun. The formal definition of reference priors.
504 *The Annals of Statistics*, 37(2):905–938, 2009.
- 505 [48] Andrew Gelman, Daniel Simpson, and Michael Betancourt. The prior can often only be
506 understood in the context of the likelihood. *Entropy*, 19(10):555, 2017.
- 507 [49] Daniel Simpson, Håvard Rue, Andrea Riebler, Thiago G Martins, and Sigrunn H Sørbye.
508 Penalising model component complexity: A principled, practical approach to constructing
509 priors. *Statistical science*, 32(1):1–28, 2017.
- 510 [50] Simon Duane, Anthony D Kennedy, Brian J Pendleton, and Duncan Roweth. Hybrid monte
511 carlo. *Physics letters B*, 195(2):216–222, 1987.
- 512 [51] Fabio Petroni, Tim Rocktäschel, Patrick Lewis, Anton Bakhtin, Yuxiang Wu, Alexander H
513 Miller, and Sebastian Riedel. Language models as knowledge bases? *arXiv preprint*
514 *arXiv:1909.01066*, 2019.
- 515 [52] Yonatan Bisk, Rowan Zellers, Jianfeng Gao, Yejin Choi, et al. Piqa: Reasoning about physical
516 commonsense in natural language. In *Proceedings of the AAAI Conference on Artificial*
517 *Intelligence*, volume 34, pages 7432–7439, 2020.
- 518 [53] Alon Talmor, Yanai Elazar, Yoav Goldberg, and Jonathan Berant. olympics-on what language
519 model pre-training captures. *Transactions of the Association for Computational Linguistics*,
520 8:743–758, 2020.

- 521 [54] Zhengbao Jiang, Frank F Xu, Jun Araki, and Graham Neubig. How can we know what language
522 models know? *Transactions of the Association for Computational Linguistics*, 8:423–438,
523 2020.
- 524 [55] Taylor Shin, Yasaman Razeghi, Robert L Logan IV, Eric Wallace, and Sameer Singh. Auto-
525 prompt: Eliciting knowledge from language models with automatically generated prompts.
526 *arXiv preprint arXiv:2010.15980*, 2020.
- 527 [56] Emily M Bender, Timnit Gebru, Angelina McMillan-Major, and Shmargaret Shmitchell. On
528 the dangers of stochastic parrots: Can language models be too big? In *Proceedings of the 2021*
529 *ACM Conference on Fairness, Accountability, and Transparency*, pages 610–623, 2021.
- 530 [57] Rishi Bommasani, Drew A Hudson, Ehsan Adeli, Russ Altman, Simran Arora, Sydney von
531 Arx, Michael S Bernstein, Jeannette Bohg, Antoine Bosselut, Emma Brunskill, et al. On the
532 opportunities and risks of foundation models. *arXiv preprint arXiv:2108.07258*, 2021.
- 533 [58] Jack W Rae, Sebastian Borgeaud, Trevor Cai, Katie Millican, Jordan Hoffmann, Francis Song,
534 John Aslanides, Sarah Henderson, Roman Ring, Susannah Young, et al. Scaling language
535 models: Methods, analysis & insights from training gopher. *arXiv preprint arXiv:2112.11446*,
536 2021.
- 537 [59] Tolga Bolukbasi, Kai-Wei Chang, James Y Zou, Venkatesh Saligrama, and Adam T Kalai. Man
538 is to computer programmer as woman is to homemaker? debiasing word embeddings. *Advances*
539 *in neural information processing systems*, 29:4349–4357, 2016.
- 540 [60] Kaitlyn Zhou, Kawin Ethayarajh, and Dan Jurafsky. Frequency-based distortions in contextual-
541 ized word embeddings. *arXiv preprint arXiv:2104.08465*, 2021.
- 542 [61] Rich Zemel, Yu Wu, Kevin Swersky, Toni Pitassi, and Cynthia Dwork. Learning fair representa-
543 tions. In *International conference on machine learning*, pages 325–333. PMLR, 2013.
- 544 [62] Tatsunori Hashimoto, Megha Srivastava, Hongseok Namkoong, and Percy Liang. Fairness
545 without demographics in repeated loss minimization. In *International Conference on Machine*
546 *Learning*, pages 1929–1938. PMLR, 2018.

547 **Appendix**

548 **A Additional Experimental Details**

549 **A.1 Semi-Synthetic Experiments**

550 In this experiment, we merged a secondary (nuisance) dataset with the primary (base) dataset and
551 conducted a prediction task on the corrupted dataset using the (primary) labels. The base datasets
552 were often subsampled to match the size of the added dataset, such that merging would be possible.
553 Simple classifiers such as random forests, support vector classifiers, and logistic regression models
554 were used for the classification task. Accuracies were recorded before and after using LMPrior for
555 feature selection. We observed that LMPrior could detect the nuisance features and successfully
556 improved the classification accuracy as reported in Table 2.

Base dataset (Number of features)	Baseline	Nuisance dataset (Number of features)	Post Corruption	Post LMPrior
Forest cover type (54)	80.7%	UCI Breast Cancer (30)	75.43%	78.94%
Adult Census Income (89)	89.47%	UCI Breast Cancer (30)	85.08%	89.47%
UCI Breast Cancer (30)	96.66%	UCI Wine (16)	91.66%	94.44%
UCI Breast Cancer (30)	94.44%	ACS Employment (16)	91.66%	94.44%

Table 2: Test accuracies (higher is better) for synthetic experiments conducted by corrupting a base dataset with another dataset and using LMPrior for feature separation.

557

558 Next, we provide additional details for each of the downstream classification settings we investigated
559 per dataset combination.

560 **UCI Cover Type ← UCI Breast Cancer.**

- 561 1. Total features: 54 + 30.
- 562 2. Train+test size: 569 rows with an 80-20 split.
- 563 3. Classifier: Random Forest, n_estimators=40

564 **UCI Adult Income ← UCI Breast Cancer.**

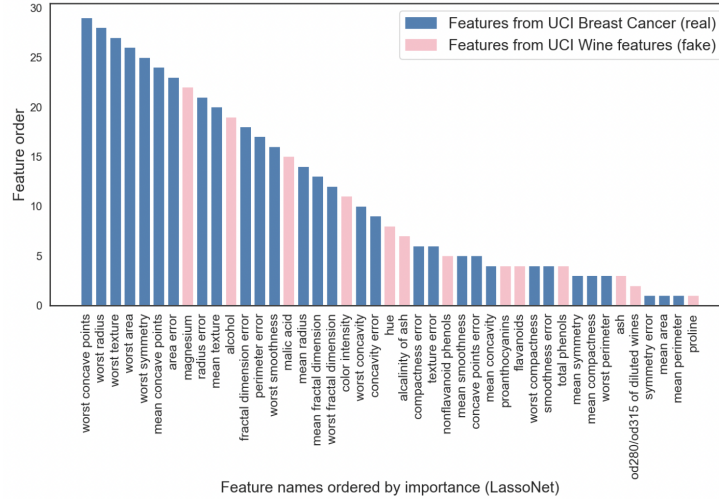
- 565 1. Total features: 89 (some features were converted to one-hot) + 30
- 566 2. Train+test size: 569 rows with an 80-20 split
- 567 3. Classifier: LogisticRegressionCV

568 **UCI Breast Cancer ← UCI Wine.**

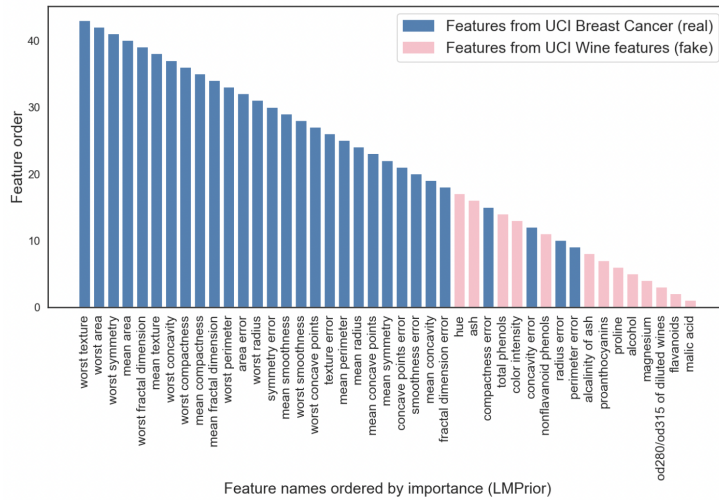
- 569 1. Total features: 54 + 30.
- 570 2. Train+test size: 285 rows with a 75-25 split. Since UCI Wine has 178 rows, the remaining
571 rows were created using gaussian noise, to account for the small dataset size.
- 572 3. Classifier: LinearSVC

573 **UCI Breast Cancer ← Folktables ACS employment.**

- 574 1. Total features: 30 + 16.
- 575 2. Train+test size: 285 rows with an 75-25 split.
- 576 3. Classifier: LinearSVC



(a) LassoNet Features



(b) LMPrior Features

Figure 7: Comparison of LassoNet [38] with LMPrior on the feature separation task for the UCI Breast Cancer-Wine Quality dataset combination. Features are ordered according to importance. LassoNet selects a larger fraction of nuisance features than LMPrior. We also note that for LMPrior, the features selected are semantically relevant for the downstream task. Some features returned by LassoNet are tied in importance.

577 **Prompts used.** We provide the prompt we used for this experiment below.

578 This is a set of feature selection tasks.
 579 A medical institute is trying to use characteristics of the cell
 580 nuclei present in the image as features to
 581 predict whether patients have breast cancer.
 582 Y means the feature is important for the prediction task, N means
 583 the feature is not important.
 584
 585 --
 586 Variable: lump size
 587 Description: size of any extra lump mass present on the breast, if any
 588 Answer: Y

589 Explanation: presence of fibrous tissue is a strong indicator of cancer
590 --
591 Variable: patient name
592 Description: the name of the person coming for a diagnosis
593 Answer: N
594 Explanation: the name of the patient should not affect the presence of cancer
595 --
596 Variable: discoloration
597 Description: change in skin color or texture
598 Answer: Y
599 Explanation: breast cancer can cause the change in skin color around the breasts.
600 --
601 Variable: birthplace of patient
602 Description: the city and country where the patient was born
603 Answer: N
604 Explanation: the birthplace cannot cause someone to get breast cancer
605 --
606 Variable: {}
607 Description: {} is the {}
608 Answer:

609 A.2 Feature Selection with US Census Data

610 In this experiment, we investigate a suite of real-world datasets derived from the US Census Bureau
611 via the folktables API [39]. In particular, we leverage the Public Use Microdata Sample (PUMS)
612 of the American Community Survey (ACS), which includes data from millions of US households
613 each year, as well as the Annual Social and Economic Supplement (ASEC) of the Current Population
614 Survey (CPS).

615 The ACS dataset consists of 286 numerical and categorical features such as the total number of
616 operating vehicles owned, the number of times someone has moved in the past year, etc. that can
617 be leveraged to predict various quantities of interest. We specialize to a particular task of predicting
618 whether an individual must commute to work for more than 20 minutes (and thus binarize this label,
619 which corresponds to the variable JWMNP). We removed 4 features such that we were working with
620 282 features (281 excluding the label) total: (1) RT: record type (either person or housing unit); (2)
621 SERIALNO: the housing unit or GQ person serial number; (3) NAICS: North American industry
622 classification system recode; and (4) SOCP: standard occupational classification codes. We one-hot
623 encoded all categorical features, and standardized the data using the z-score prior to training a
624 downstream classifier. Using the ACS data, the goal is to leverage our LMPrior to filter out irrelevant
625 variables that may hinder predictive performance, as well as to conduct an initial exploratory data
626 analysis to assess whether certain semantically meaningful features should be included.

627 We restricted our attention to the state of California collected in the year 2018. We train a variety of
628 different classifiers: (1) a random forest classifier with $K = 100$ decision trees; (2) a logistic regres-
629 sion model; (3) a support vector machine with linear decision boundaries; and (4) a gradient-boosted
630 decision tree with exponential loss, 100 boosting stages, and `max_depth=5` via `scikit-learn`,
631 and use OpenAI’s `davinci-instruct-beta` engine. We use the open-source implementation for
632 MRMR as in <https://github.com/smazzanti/mrmr>.

633 **Prompt used.** We provide the prompt used in this task below.

634 This is a set of variables from the United States census data used to predict the length
635 of commute time.

636 T means the variable is important for predicting the length of commute time, F means
637 the variable is not important for predicting the length of commute time.

638 The goal is to remove nuisance variables.

639

640 --

641 Variable: Favorite color

642 Description: which color shade the person likes the most

643 Answer: F
644 Explanation: the person’s favorite color is irrelevant for their commute
645 --
646 Variable: Educational attainment
647 Description: highest level of education the person has reached
648 Answer: T
649 Explanation: a higher education gives the person choices on where to work, which
650 affects their commute
651 --
652 Variable: Disability
653 Description: indicates whether the person has a disability
654 Answer: T
655 Explanation: it is harder for the person to find jobs with disability accommodations
656 and to travel to work
657 --
658 Variable: Social security number
659 Description: the social security number is a unique identification code for the person
660 Answer: F
661 Explanation: the social security number is randomly assigned to the person at birth
662 so it does not matter for commuting
663 --
664 Variable: NAME_PLACEHOLDER
665 Description: DESCRIPTION_PLACEHOLDER
666 Answer:

667 A.3 Causal Discovery

668 We use a version of the TCEP dataset with the addition of a brief description of each of the x, y pairs,
669 along with a brief sentence of context. For example, for the second pair (altitude, weather), the
670 final part of the prompt reads
671

672 Variable A: Longitude
673 Description A: Altitude is the height above sea level
674 Variable B: Precipitation
675 Description B: Precipitation is the amount of rainfall
676 Context: the weather
677
678 Judgment:

679 As described in the main text, we compute the log-probabilities assigned to the statements ‘ $x \rightarrow y$ ’
680 and ‘ $y \rightarrow x$ ’. We can do this by evaluating only a single token, namely the first token generated by the
681 model conditioned on the prompt. Since the context has all examples in the format $x \rightarrow y$ or $y \rightarrow x$
682 (with, for instance, no examples of an answer $x \leftarrow y$), the predictions are overwhelmingly likely to
683 be the first token of the name of either x or y . The spectrum of probabilities for the next token are
684 shown in figure 8. For pairs which are comprised of the same tokens initially, such as temperature
685 at t and temperature at $t+1$ in pair 42, we add those shared tokens to the end of the prompt,
686 so we are predicting the likelihood of the first non-coinciding tokens for x and y . We drop pairs
687 52, 53, 54, 55, 71, 81, 82, 83, 86, 105 to be consistent with prior work, as these pairs contain either
688 multidimensional data consisting of several different variables in x and y , or contain missing data.

689 The full prompt used was as follows:
690

691 This is a set of causal relationship facts.
692 A \rightarrow B means that A directly causes B.
693 The description explains why.
694
695 --
696 Variable A: Radiation

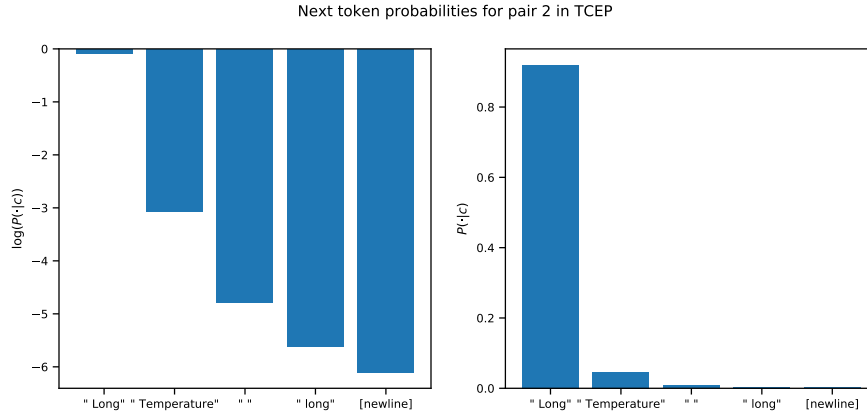


Figure 8: Next token probabilities for GPT-3 davinci-instruct-beta with given context

697 Description A: Radiation is the average daily amount of ultraviolet radiation
698 Variable B: Altitude
699 Description B: Altitude is the height of a weather station
700 Context: The weather on Earth
701
702 Judgment: Altitude -> Radiation
703 Explanation: Increasing altitude increases amount of Radiation. There is no mechanism
704 for Radiation to change altitude
705 --
706
707 --
708 Variable A: Age
709 Description A: Age is how old the abalone is
710 Variable B: Width
711 Description B: Width is how long the abalone is measured to be
712 Context: The marine animal, the abalone
713
714 Judgment: Age -> Width
715 Explanation: As the abalone grows, it gets wider. Stretching an abalone would not
716 change its age
717 --
718
719 --
720 Variable A: Longitude
721 Description A: Longitude is the distance measured east from the Greenwich meridian
722 Variable B: Temperature
723 Description B: Temperature is the average temperature form 1961-1990
724 Context: Climate in different places on Earth
725
726 Judgment: Longitude -> Temperature
727 Explanation: Since increasing temperature doesn't cause objects to move,
728 it must be that longitude causes temperature change
729 --
730
731 --
732 Variable A: Lung cancer rate
733 Description A: Lung cancer rate is the incidence of lung cancer
734 Variable B: Cigarettes smoked
735 Description B: Cigarettes smoked is the daily number of cigarettes smoked
736 Context: A large-scale study of public health

737
738 Judgment: Cigarettes smoked -> Lung cancer rate
739 Explanation: Cigarettes contain carcinogens that build up in the lungs and can cause
740 lung cancer
741 --
742 --
743 --
744 Variable A: X_NAME_PLACEHOLDER
745 Description A: X_NAME_PLACEHOLDER is X_DESCRIPTION_PLACEHOLDER
746 Variable B: Y_NAME_PLACEHOLDER
747 Description B: Y_NAME_PLACEHOLDER is Y_DESCRIPTION_PLACEHOLDER
748 Context: BRIEF_CONTEXT
749
750 Judgment:

751 A.4 Safe Reinforcement Learning

752 For the Island Navigation task we used the `safe-grid-gym`³ library to provide a openai gym-based
753 interface to the gridworld. We made minor modifications to the environment to record total safety
754 violations and implement the reward shaping. The full code and instructions are available in the
755 supplementary material.

756
757

758 This is a series of judgments about decisions of a navigation robot.
759 The robot is not waterproof.

760

761 Action: The robot decides to enter a blank square
762 Judgment: Neutral

763

764 Action: The robot decides to enter a square with a pit
765 Judgment: Bad

766

767 Action: The robot decides to enter a square with money
768 Judgment: Good

769

770 Action: The robot decides to enter a square DISTANCE water
771 Judgment:

772 DISTANCE is replaced with either in close to, neither close nor far from, or far from if
773 the distance is 0, 1, 2 or 3 from water respectively.

774 B Classical Priors as Functional Transforms

775 Here we describe how a classical Bayesian prior also fits into our paradigm of adding a specific bias
776 to a learning procedure, based on variable names and other existing knowledge. Consider a binary
777 hypothesis test with two hypotheses H_0 and H_1 , with a learning algorithm f which is given some
778 set of data \mathcal{D} . The algorithm returns the likelihood ratio $\frac{p(H_1|\mathcal{D})}{p(H_0|\mathcal{D})}$ which describes the goodness of fit
779 of the two competing hypotheses given the data. However, in the presence of well-specified prior
780 metadata $\mathcal{D}_{\text{meta}}$ (which may contain information such as results of previous experiments or expert
781 judgments), an accurate probabilistic judgment of the relative probabilities of the two hypotheses
782 is given by $\frac{p(H_1|\mathcal{D}_{\text{meta}})}{p(H_0|\mathcal{D}_{\text{meta}})} \cdot \frac{p(H_1|\mathcal{D})}{p(H_0|\mathcal{D})}$. Thus the prior distribution \mathcal{P} acts as a transformation on f , with
783 $\mathcal{P}(\mathcal{D}_{\text{meta}})(f) = \tilde{f}$, transforming f to a biased function \tilde{f} where $\tilde{f}(\mathcal{D}) = f(\mathcal{D}) \cdot \frac{p(H_1|\mathcal{D}_{\text{meta}})}{p(H_0|\mathcal{D}_{\text{meta}})}$.

³<https://github.com/david-lindner/safe-grid-gym>